Biogeochemical Layering and Transformation of Particulate Organic Carbon in the Tropical Northwestern Pacific Ocean Inferred from $\delta^{13}C$

Authors

Detong Tian[1,3], Xuegang Li[1,2,3,4*], Jinming Song[1,2,3,4*], Jun Ma[1,2], Huamao Yuan[1,2,3,4], Liqin Duan[1,2,3,4]

Affiliations

[1]CAS Key Laboratory of Marine Ecology and Environmental Sciences, Institute of Oceanology, Chinese Academy of Sciences, Qingdao 266000, China

[2]Laboratory for Marine Ecology and Environmental Science, Qingdao Marine Science and Technology Center, Qingdao 266237, China

[3]University of Chinese Academy of Sciences, Beijing 100049, China

[4]Center for Ocean Mega-Science, Chinese Academy of Sciences, Qingdao 266000, China

Corresponding to: Xuegang Li (lixuegang@qdio.ac.cn) and Jinming Song (jmsong@qdio.ac.cn).

Abstract. Particulate organic carbon (POC) serves as the main carrier of the biological pump and determines its transmission efficiency, yet the transformation processes of POC remain incompletely understood. This study reports the vertical distribution of POC, dissolved inorganic carbon (DIC), $\delta^{13}C$-POC, and $\delta^{13}C$-DIC in the tropical Northwestern Pacific Ocean (TNPO). The research identified three distinct biogeochemical layers governing POC transformation: the POC rapid synthesis-degradation layer (RSDL, 0-300 m), the net degradation layer (NDL, 300-1,000 m), and the stable layer (SL, 1,000-2,000 m). From the top to the bottom of the RSDL, $\delta^{13}C$-POC values decreased by an average of 2.23‰, while the carbon-to-nitrogen ratios (C:N) increased by an average of 2.3:1, indicating the selective degradation of POC. In the NDL, $\delta^{13}C$-POC and $\delta^{13}C$-DIC exhibited a significant negative correlation (r = 0.43, $p < 0.05$), indicating a net transformation of POC to DIC. In the SL, POC proved to be resistant to degradation, with POC exhibiting the highest C:N (15:1 on average) and the lowest $\delta^{13}C$-POC values (average -27.71‰).

1 Introduction

As the most significant carbon reservoir on the earth's surface, the ocean absorbs about 2.6 billion tons of carbon dioxide (CO_2) from the atmosphere each year, accounting for 25% of global anthropogenic CO_2 emissions (Friedlingstein et al., 2023). After entering the ocean, CO_2 initially dissolves in seawater, forming dissolved inorganic carbon (DIC). Subsequently, phytoplankton and photosynthetic bacteria at the ocean surface convert it into organic carbon through photosynthesis. The majority of carbon in the ocean is in the form of DIC, constituting over 98% of the total carbon content, with the remaining 2%

existing as POC and dissolved organic carbon (DOC). Despite being in minimal quantities, POC can be transported to the deep ocean through the biological pump and buried for thousands of years. This process of carbon sequestration aids in the absorption of CO_2 by the ocean, contributing to the regulation of atmospheric CO_2 levels (Longhurst and Glen Harrison, 1989; Turner, 2015). Organic matter produced from the euphotic layer is the primary food source for heterotrophic communities in the dark ocean (Smith et al., 2008); once POC is exported from the euphotic layer, microorganisms rapidly utilize it, releasing DIC (Song, 2010).

Some studies have shown that unstable components such as proteins and carbohydrates in POC are preferentially degraded by microorganisms (Eadie and Jeffrey, 1973). However, conducting detailed quantitative analyses of each POC component in actual investigations is challenging, necessitating the use of alternative indicators to demonstrate selective degradation. ~~The~~ One generally accepted indicator is the carbon-to-nitrogen ratios (C:N) due to inherent differences in the C:N of various compounds in POC (Morales et al., 2021). Thus, changes in the C:N during degradation can signify the selective degradation of POC. Nevertheless, the composition of POC is highly complex, and the C:N of its different components are not absolute. For example, lipids typically have a higher C:N than proteins, but the opposite can also occur (Sannigrahi et al., 2005; Hernes and Benner, 2002). Therefore, relying solely on the C:N to reflect the selective degradation process of POC has significant limitations. Although the vital activities of the microbial community in the dark ocean are predominantly driven by heterotrophic respiration (Herndl et al., 2023), many autotrophic organisms use chemical energy to synthesize POC. Compelling evidence indicates that chemoautotrophy plays a substantial role in the fixation of DIC in the minimum oxygen zone (OMZ) (Reinthaler et al., 2010) and the deeper ocean (Passos et al., 2022; Walsh et al., 2009). Consequently, there is a continuous conversion of POC and DIC throughout the ocean water column. Exploring the degradation and synthesis of POC in the ocean is imperative to enhance our comprehension of the biological pump processes.

The DIC in seawater primarily occurs in four chemical forms: H_2CO_3, HCO_3^-, CO_3^{2-}, and CO_2. In comparison, the composition of POC is more complex. POC comprises various organic compounds originating from living organisms such as phytoplankton, zooplankton, and microorganisms. It also encompasses fecal particles, cell fragments, and diverse organic substances from external sources. Only a small fraction of the POC has been accurately identified in terms of molecular structures (Kharbush et al., 2020). As the depth increases, the readily degradable components in POC are used up, leading to a more intricate structure of the remaining POC through the transformation process. The remaining refractory POC is even more difficult to identify (Lee et al., 2000). Therefore, it becomes challenging to study the chemical characteristics of POC and its transformation process from itself. The $\delta^{13}C$ is a crucial indicator that can reveal the origin, migration, and transformation of POC, making it significantly important in the investigation of the marine carbon cycle (Ding et al., 2020; Jeffrey et al., 1983). Compared with POC concentrationmolecules, $\delta^{13}C$-POC provides a more accurate reflection of the chemical properties of the POC pool and the migration and transformation processes of POC (Close and Henderson, 2020). Similarly, $\delta^{13}C$-DIC can offer insights into important processes within the ocean carbon cycle. As POC settles, it undergoes a series of biogeochemical processes, including synthesis, degradation, and adsorption. Therefore, the isotope fractionation effect in POC is strong, resulting in significant differences in $\delta^{13}C$-POC values at different depths. In contrast, the fractionation of $\delta^{13}C$-DIC is subject to fewer influencing factors, and the DIC concentration in the ocean is notably high, thereby engendering minimal variability in $\delta^{13}C$-DIC values across the ocean water column (Jeffrey et al., 1983). Therefore, $\delta^{13}C$-DIC is more sensitive to the fractionation effect in the ocean carbon cycle. Even slight variations in the $\delta^{13}C$-DIC values can reflect significant processes involved in the migration and transformation of POC (Quay and Stutsman, 2003). Through the analysis of $\delta^{13}C$-POC and $\delta^{13}C$-DIC values, we can enhance our comprehension of the intricate composition, transport, and alteration mechanism of POC, providing us with a more profound insight into the dynamic transformations within the ocean biological pump.

The tropical Northwestern Pacific Ocean (TNPO) is characterized by intricate current patterns and water mass distributions (Hu et al., 2015; Schönau et al., 2022), and it is also known for the highest surface seawater temperatures globally (Jia et al., 2018). High temperatures facilitate the respiration of by heterotrophic organisms, promoting the formation of biological hotspots and ultimately enhancing material circulation and energy flow in the upper ocean (Guo et al., 2023a; Iversen and Ploug, 2013). The air-sea interaction within the TNPO is highly dynamic, exhibiting a shift from being a carbon sink to a carbon source as it extends from higher to lower latitudes (Takahashi et al., 2009; Wu et al., 2005). The complex hydrological characteristics, rapid elemental cycle, and frequent air-sea exchange render the TNPO an ideal laboratory for exploring the ocean carbon cycle. In this research, we collected seawater and particulate matter samples at six stations in the core and boundary regions of the TNPO, and the relationship between DIC, POC, and their stable carbon isotopes was comprehensively analyzed to enhance our understanding of the POC transformation process and the ocean carbon cycle process.

2 Sampling and Methods

The samples were collected in the TNPO during an expedition on R/V *Kexue* from March to April 2022. A total of 6 stations were set up: EQ-6 (150.99° E, 0.00° N, 1944 m), E142-3 (140.99° E, 12.01° N, 4091 m), E142-7 (140.99° E, 15.99° N, 4725 m), E142-11 (140.99° E, 20.00° N, 462 4m), E142-13 (142.04° E, 0.00° N, 3382 m) and E142-19 (141.99° E, 6.01° N, 2580 m) (Fig. 1). The 12-L Niskin bottles (KC-Denmark, Denmark) mounted on a Conductivity-Temperature-Depth (CTD, Sea-bird SBE911, United States) rosette ~~was~~ were used to obtain water samples from the vertical profile of 0-2,000 m at each station for analysis of temperature, salinity, dissolved oxygen (DO), POC, δ^{13}C-POC, particulate nitrogen (PN), DIC, δ^{13}C-DIC, and chlorophyll a (Chl-*a*). The specific sampling and analysis methods are as follows.

Temperature and salinity: The temperature and salinity were measured by CTD (Sea-bird SBE911, United States) in situ during sampling.

DO: DO was determined in situ using the Winkler method with a measurement precision of 2.2×10^{-3} μmol/L. At each depth, we collected samples in 50 mL brown bottles, added manganese sulfate and alkaline potassium iodide to fix the oxygen, then titrated the released iodine with sodium thiosulfate to calculate DO concentrations~~Water samples were collected, fixed, and titrated according to the classic Winkler method, the precision of which was 2.2×10^{-3} μmol/L~~ (Bryan et al., 1976; Zuo et al., 2018). The discrete DO samples were used to calibrate the DO concentration data obtained by the CTD sensor.

POC, δ^{13}C-POC, and PN: Particle samples were obtained by filtering 2-5 L of seawater onto a GF/F glass filter (0.7 μm, Whatman) that had been combusted in a muffle furnace (450°C, 4 h) and acid-soaked (0.5 M hydrochloric acid (HCl), 24 h). The filter was treated with HCl to remove inorganic carbonates and oven-dried at 60°C. After collection, samples were stored below -20 ℃ until laboratory analysis. Afterward, POC, PN concentration, and δ^{13}C-POC values were analyzed using an elemental analyzer and an isotope mass spectrometer (Thermo Fisher Scientific Flash EA 1112 HT-Delta Ⅴ Advantages, United States) with an accuracy of ± 0.8‰ and ± 0.2‰, respectively. Standard reference materials were used to calibrate δ^{13}C and POC, PN measurements, including USGS64 (δ^{13}C = -40.8 ± 0.04‰, C%

= 31.97%, N% = 18.65%, Indiana University), USGS40 ($\delta^{13}C$ = -26.39 ± 0.04‰, C% = 40.8%, N% = 9.52%, Geological Survey, United States), and Urea #2a ($\delta^{13}C$ = -9.14 ± 0.02‰, C% = 20%, N% = 46.67%, Indiana University). We implemented a quality control protocol by randomly inserting a certified reference material after every 10 samples. The measured values of these reference materials were subsequently plotted against the calibration curve to monitor and verify instrument stability throughout the analytical process (Ma et al., 2021).

DIC and $\delta^{13}C$-DIC: Sampling was performed using a 50 ml glass bottle. After the water sample overflowed, 1 ml of the sample was taken out with a pipette and then fixed with saturated mercuric chloride solution to remove the influence of biological activity. After collection, samples were stored in refrigerator at 4°C for later laboratory measurement of DIC concentration using a total DIC analyzerThe DIC concentration was measured using a DIC analyzer (Apollo SciTech AS-C3, United States) with an accuracy of ± 0.1% (Ma et al., 2020). For calibration, certified reference material (Batch 144, 2031.53 ± 0.62 μmol/kg) provided by the Scripps Institution of Oceanography (University of California, San Diego) was used. $\delta^{13}C$-DIC values automatic: Automatic analysis was performed using a Thermo Delta-V isotope ratio mass spectrometer (ThermoFisher Scientific MAT 253Plus, United States). For calibration, certified reference materials for $\delta^{13}C$-DIC were used, including GBW04498 ($\delta^{13}C$ = -27.28 ± 0.10‰), GBW04499 ($\delta^{13}C$ = -19.58 ± 0.10‰), and GBW04500 ($\delta^{13}C$ = -4.58 ± 0.12‰), all provided by the Institute of Geophysical and Geochemical Exploration (Chinese Academy of Geological Sciences). We inserted a reference standard every 10 samples, using its measured values to verify instrument stability via the calibration curve.

Chl -*a*: 2 L of water sample after zooplankton removal was filtered onto pre-combusted (450°C for 5 hr) GF/F filters (0.7 μm, Whatman), and placed in the refrigerator at −20°C before measurement. In the laboratory, the filters were extracted with 90% propanol for 12-24 h, and the concentration was measured using a fluorescence photometer (Turner Designs, United States) For calibration, Chlorophyll a analytical standard (purity ≥ 95.0%) provided by Sigma-Aldrich (SIAL, St. Louis, MO, United States) were used. (Ma et al., 2020).

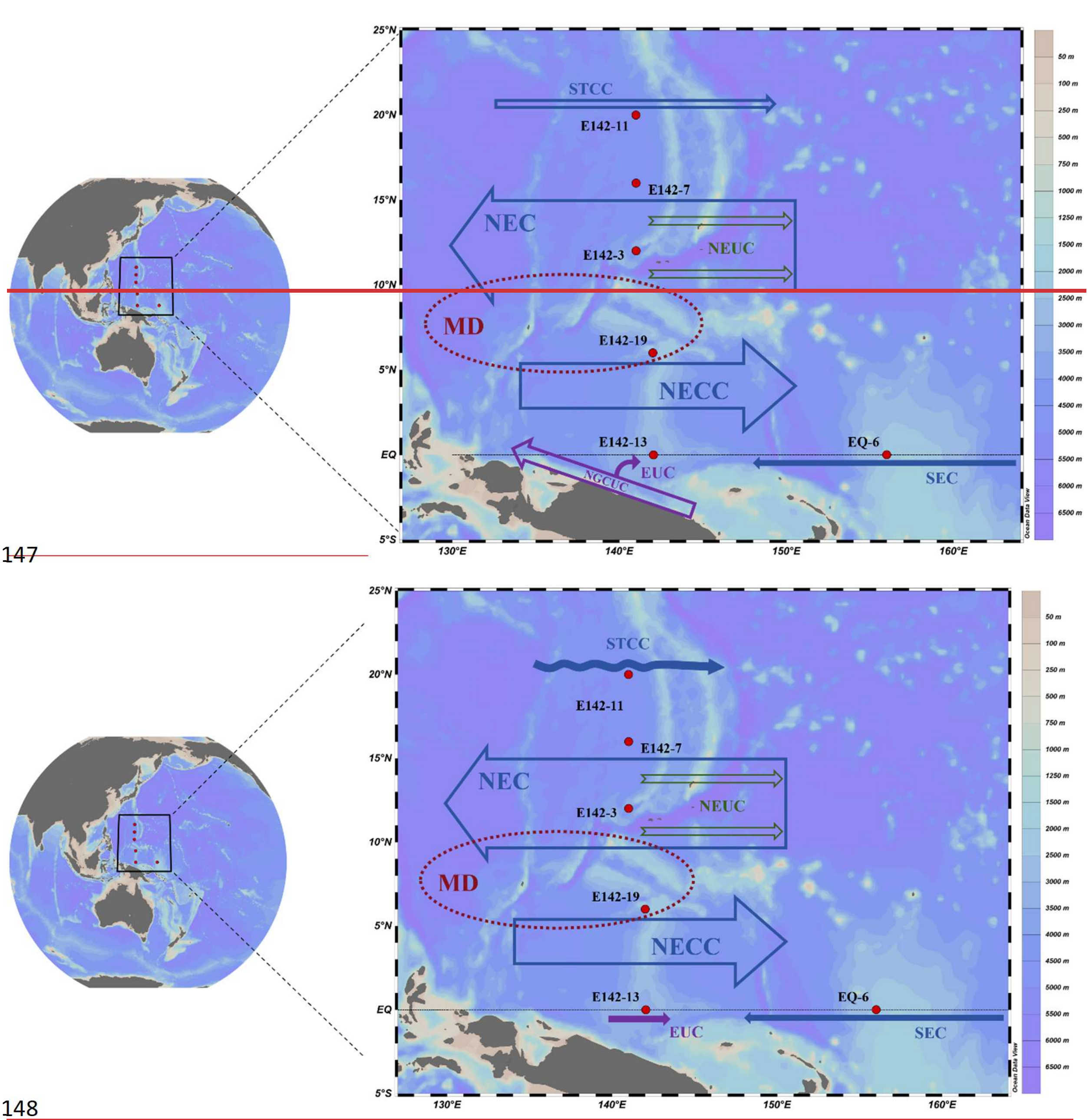

Figure 1. TPWO sampling stations (red dots in the figure) and ocean current distribution. In the figure, blue represents the ocean currents from the surface to the bottom of the thermocline, mainly STCC, NEC, NECC, and SEC; green represents the ocean currents in the subthermocline, mainly NEUC; purple represents the ocean currents from the bottom of the thermocline to the subthermocline, mainly EUC.

3 Results and Discussion

3.1 Hydrological Characteristics

Except for station E142-11, the remaining five stations are all located at the Western Pacific Warm Pool (WPWP). The SST of the five stations in the warm pool area was higher, averaging 29.01 ± 0.67 ℃, while station E142-11 had a lower SST of 25.02 ℃. The strong seawater stratification in the study area restricted the movement of nutrient-rich water from the deep to the upper ocean, resulting in the region showing oligotrophic characteristics (Radenac et al., 2013). Therefore, the Chl-*a* concentration in at the deep chlorophyll maximum layer depth (DCMD) was notably low, with an average of only 0.24 ± 0.04 μg/L. Based on the fluorescence intensity measured by the CTD in-situ fluorescence sensor, we calculated the Primary Production Zone Depth (PPZD), which is the depth where the fluorescence intensity drops to 10% of its maximum value above this depth (Owens et al., 2015). Additionally, the Mixed Layer Depth (MLD) at each station was determined using the temperature threshold method (Table 1) (Thompson, 1976). The results indicate that the PPZD at each station is deeper than the MLD, suggesting that the POC generated at these stations does not undergo particularly complex physical mixing after its formation (Buesseler et al., 2020).

Table 1. The water depth (WD), the PPZD, the MLD, the deep chlorophyll maximum layer depth (DCMD) and the Chl-*a* at DCMD for each station.

Station	Longitude °E	Latitude °N	WD m	PPZD m	MLD m	DCMD m	Chl-*a* μg/L
EQ-6	155.99	0.00	1944	129	65	50	0.31
E142-3	141.00	12.01	4091	216	102	140	0.19
E142-7	141.00	16.00	4725	204	68	150	0.25
E142-11	140.99	20.00	4624	203	42	90	0.21
E142-13	142.04	0.00	3382	165	45	90	0.25
E142-19	142.00	6.01	2580	170	109	100	0.21

Based on the relationship between potential temperature and salinity (θ-S) (Fig. 2), eight water masses in the study area were identified: North Pacific Tropical Surface Water (NPTSW), North Pacific Subsurface Water (NPSSW), North Pacific Subtropical Mode Water (NPSTMW), North Pacific Intermediate Water (NPIW), North Pacific Deep Water (NPDW), as well as Equatorial Surface Water (ESW), South Pacific Subsurface Water (SPSSW) and South Pacific Intermediate Water (SPIW). In the upper ocean (0-300 m), we found that both NPTSSW and SPSSW exhibited high salinity characteristics. The salinity of NPTSSW was distributed between 34.66 and 35.01, while the salinity of SPSSW was distributed between 35.15 and 35.65. In addition, as the water depth increased, the temperature of NPTSSW and SPSSW decreased significantly, with NPTSSW dropping from 27.18℃ to 16.21℃ and SPSSW dropping from 29.23℃ to 14.81℃. The representative water mass in the middle ocean (300-

1000 m) is NPIW, which is characterized by a rapid decrease in temperature (11.44-5.57℃) and a slight increase in salinity (~0.3) with increasing water depth. The representative water mass in the deep ocean (1000-2000 m) is NPDW, which has stable properties and slight changes in salinity and temperature. Notably, the water mass distribution at station E142-19 is quite special. Ranging from the subsurface to the deep layer, the water mass properties of this station are relatively stable, showing low-salinity and low-temperature characteristics. This is attributed to the intrusion of both North Pacific Intermediate Water (NPIW) and South Pacific Intermediate Water (SPIW) into the station in the mid-ocean region. Additionally, the station is situated within the MD upwelling area, where strong upwelling transports low-temperature, low-salinity North Pacific Deep Water (NPDW) from the bottom to the upper layer, enhancing seawater exchange. Consequently, the water at station E142-19 comprises a mixture of diverse water masses (MW).

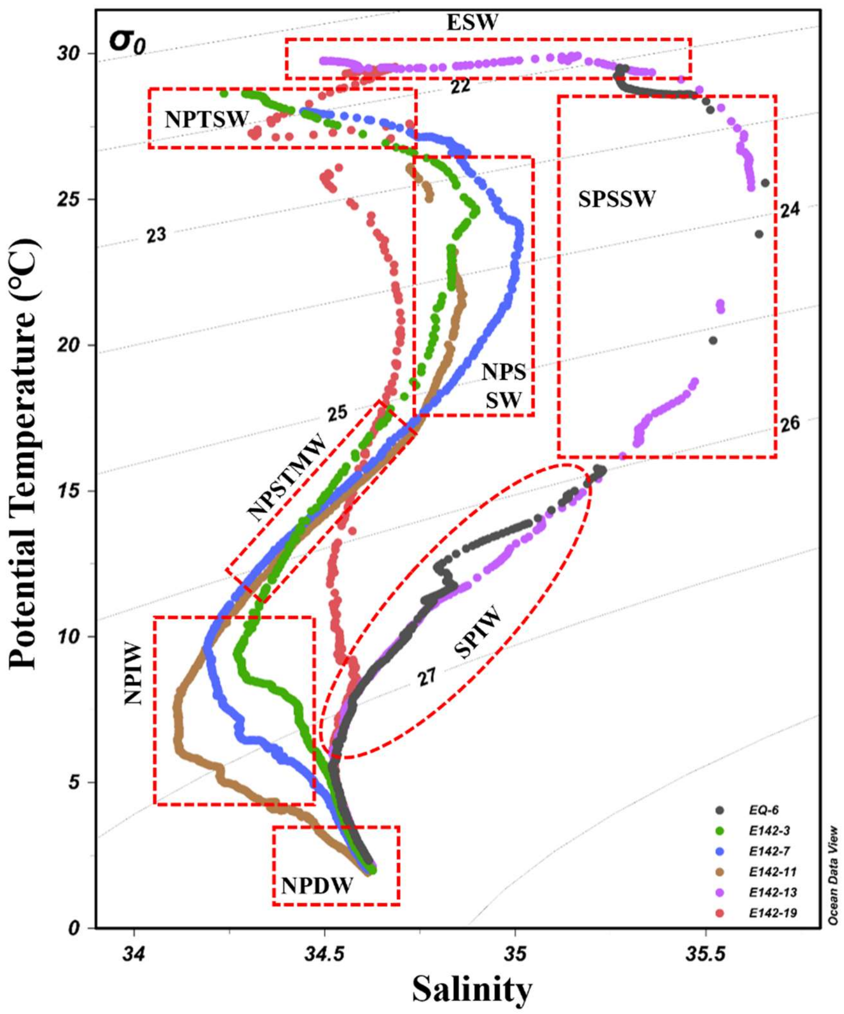

Figure 2. Relationship between potential temperature (θ) and salinity (S) at each sampling station. The water mass distribution is marked with a dotted line.—

The study area is traversed by six major ocean currents: the South Equatorial Current (SEC), the North Equatorial Current (NEC), the North Equatorial Undercurrent (NEUC), the Subtropical Countercurrent (STCC), the Equatorial Undercurrent (EUC) and the North Equatorial Countercurrent (NECC). Among them, the SEC flows from east to west along the equator and is characterized by high temperature and low salinity, notably impacting station EQ-6. The NEC is a major westward current in the study area, accompanied by a series of eastward undercurrents of NEUC in its lower part; stations E142-3 and E142-7 are mainly affected by them. The STCC is characterized by a multi-eddy structure that flows eastward in the subtropical region of the North Pacific and notably impacts station E142-11. The EUC is a strong eastward current rich in oxygen and nutrients, which are present in the subsurface layer of the equatorial Pacific, forming the main body of the thermocline of this area; station E142-13 is deeply affected by it. The NECC is an important current in the tropical Pacific equatorial current system, transporting warm pool water from the western Pacific to the eastern Pacific; Station E142-19 is mainly affected by it. Furthermore, the area features a substantial upwelling system known as the Mindanao Dome (MD), greatly impacting Station E142-19, situated southeast of the MD.

3.2 Vertical distribution characteristics of POC and δ^{13}C-POC

The average POC concentration from the surface to the deep chlorophyll maximum layer (DCM, 0-150 m) of the six stations was: E142-19 (34.12 ± 3.53 μg/L) > E142-13 (31.90 ± 3.19 μg/L) > EQ-6 (31.32 ± 5.27 μg/L) > E142-3 (27.77 ± 4.78 μg/L) > E142-7 (27.43 ± 1.35 μg/L) > E142-11 (26.81 ± 2.25 μg/L). Since the nutrient concentration in ESW and SPSSW is higher than that in NPTSW and NPTSSW, ~~The~~the surface POC concentrations at stations E142-13 and EQ-6 were slightly higher than those at other stations. However, the surface POC concentration at station E142-19 was the highest among the six stations because the robust upwelling of MD brought rich nutrients to the surface seawater, alleviating the nitrogen nutrient limitation of the surface water at this station (Gao et al., 2021).

The POC concentration of each station demonstrated a decreasing trend with increasing water depth and tended to remain stable in the deep ocean (> 1,000 m) (~~Fig. 2~~). The most significant drop in POC concentration occurred between the DCM and 600 m (Fig. 3). The seawater within this depth range was abundant in POC and also exhibited relatively high temperature and DO concentration, which likely enhanced the metabolic activities of heterotrophic organisms, thereby accelerating their utilization of POC (Iversen and Ploug, 2013; Sun et al., 2021). The aerobic degradation of POC led to a significant consumption of DO. Therefore, the change in DO in this water layer was consistent with the change of POC concentration (~~Fig. 2~~Fig. 3). It could be inferred that the rapid degradation of POC contributes to the accelerated formation of the oxygen cline. Since the microbial life activities below the oxygen cline were still active, leading to the continued consumption of DO through POC degradation, the DO could not be replenished in time. As a result, the low oxygen zone (where DO < 100 μmol/L) emerged in the middle ocean at all stations (~~Fig. 2~~Fig. 3). However, the hypoxic conditions observed at station E142-13 were comparatively less pronounced than those observed at other stations (~~Fig. 2~~Fig. 3). This can be attributed to the consistent transport of oxygen and nutrient-rich seawater by the EUC to this station, facilitating oxygen replenishment and mitigating deoxygenation (Brandt et al., 2021).

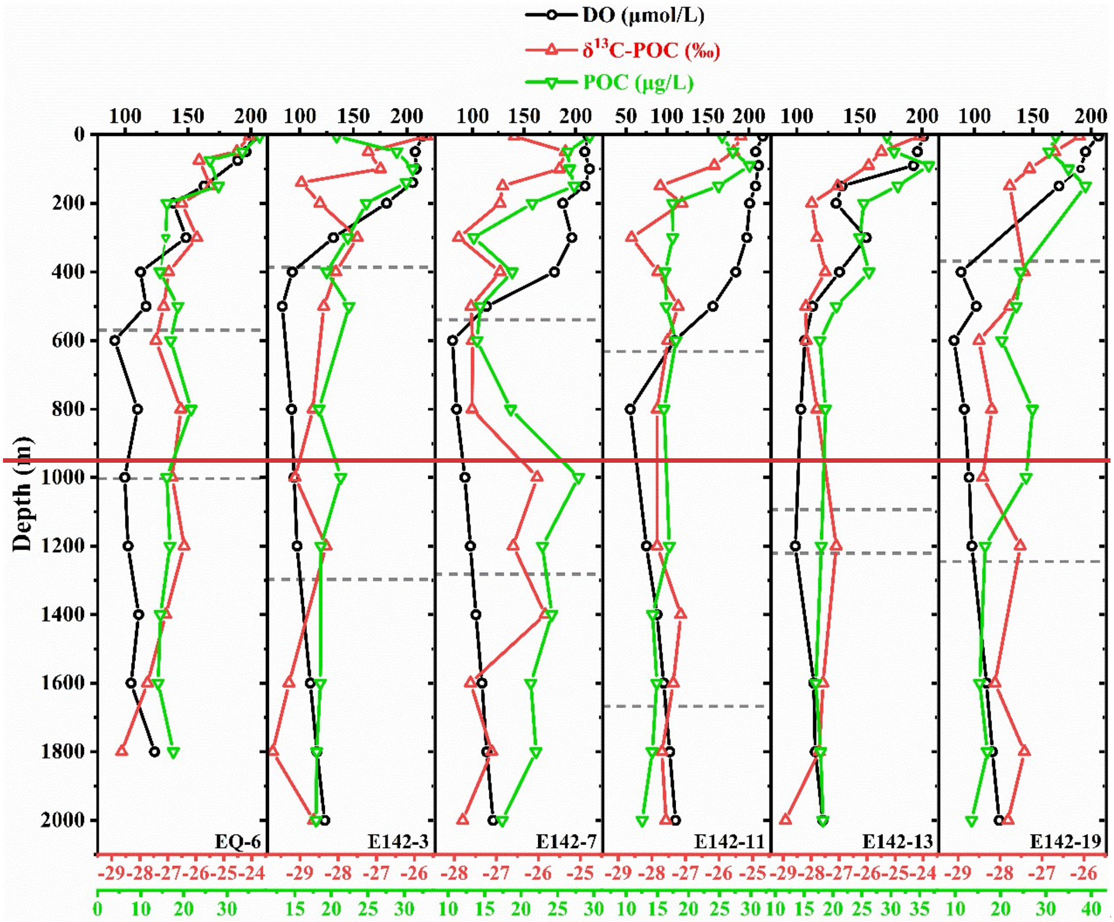
DO (μmol/L)
δ13C-POC (‰)
POC (μg/L)
Depth (m)
EQ-6
E142-3
E142-7
E142-11
E142-13
E142-19

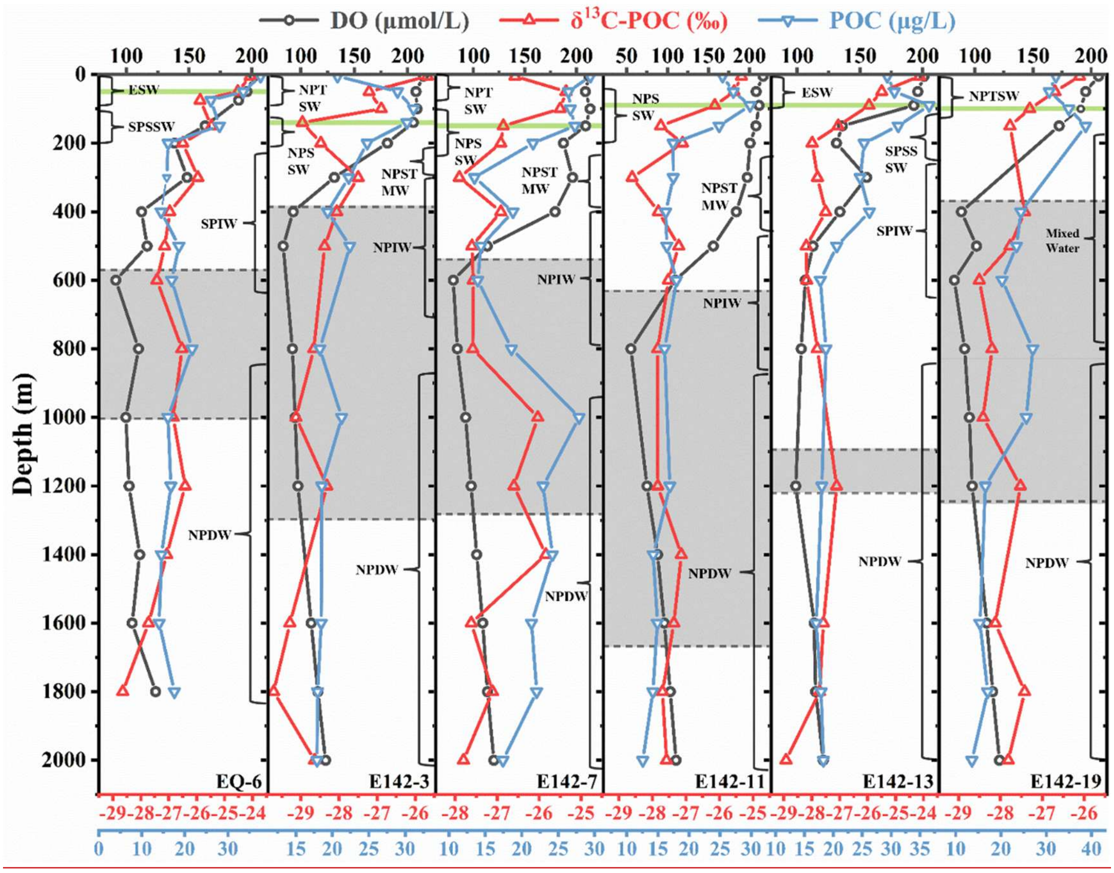
DO (μmol/L)
δ13C-POC (‰)
POC (μg/L)
Depth (m)
ESW
SPSSW
SPIW
NPDW
NPT SW
NPS SW
NPIW
NPST MW
NPS SW
NPTSW
SPSS SW
Mixed Water
EQ-6
E142-3
E142-7
E142-11
E142-13
E142-19

Figure 2Figure 3. Vertical distribution of DO concentration, δ^{13}C-POC values, and POC concentration at each sampling station. The gray areadotted line marks the hypoxic zone with DO = 100 μmol/L as the boundary. The green line represents the DCM depth.

The vertical distribution of δ^{13}C-POC values closely resembles that of POC concentration (Figs. 2, 3a). This similarity suggests that specific ^{13}C-enriched components may be preferentially degraded during POC degradation. Although the molecular composition of oceanic POC cannot be fully identified, it is generally understood to primarily consist of lipids, amino acids, carbohydrates, nucleic acids, and a small number of heterogeneous components (Kharbush et al., 2020). The metabolic activity of amino acids and carbohydrates is higher than lipids, leading microorganisms to preferentially use these compounds as energy sources, enriching lipids in POC (Hwang et al., 2006; Jeffrey et al., 1983). Previous studies have reported that during the degradation of POC, the carbon isotope fractionation characteristics of amino sugar monomers closely align with changes in δ^{13}C-POC values (Guo et al., 2023b). Moreover, several studies have highlighted that the carbon isotopic composition of lipid monomers does not exhibit significant depletion during POC degradation; in fact, it may even show a trend of enrichment (Close et al., 2014; Häggi et al., 2021). These observations further indicates the preferential degradation of amino acids and carbohydrates in POC. On the other hand, compared with lipids, amino acids and carbohydrates exhibit higher δ^{13}C values (Hayes, 1993; Hwang and Druffel, 2003; Schouten et al., 1998). When large quantities of amino acids and carbohydrates undergo selective degradation, the residual POC will show low δ^{13}C value characteristics. Therefore, as POC is continuously consumed in the water column, the δ^{13}C-POC values will gradually decrease. In addition, lipids have a low nitrogen content in comparison to amino acids and carbohydrates, leading to a relatively high C:N (Morales et al., 2021). Our findings demonstrated a strong negative correlation between δ^{13}C-POC values and C:N (Fig. 3Fig. 4b), which implied that as the water depth increases, δ^{13}C-POC values decreases while the C:N in the remaining POC increases. This suggests that selective degradation of POC occurs in our study, during which amino acids and carbohydrates in the POC were preferentially removed, resulting in a relative increase in the proportion of lipids in the remaining POC (Druffel et al., 2003; Guo et al., 2023a). However, it is noteworthy that in the upper ocean (0-300 m), although there is a significant negative correlation between δ^{13}C-POC values and C:N ratios ($p<0.05$), no significant correlation is observed between δ^{13}C-POC values and POC concentration ($p>0.05$) (Fig. 4a). This suggests that the fractionation of δ^{13}C-POC at this depth layer is not entirely controlled by selective degradation. Photosynthesis exerts a certain influence on the fractionation of δ^{13}C-POC within this depth range, primarily manifested as an increase in photosynthetic carbon isotope fractionation with depth, leading to a decrease in δ^{13}C-POC values. In a study conducted in the subtropical North Atlantic, the photosynthetic carbon isotope fractionation increased by 5.6‰ from the upper to the lower euphotic zone, while the δ^{13}C values of the photosynthetic product, phytol, decreased by 6.3‰ (Henderson et al., 2024). Therefore, although the process of selective degradation significantly affects the fractionation of δ^{13}C-POC, it is still necessary to consider the regulatory effects of other processes in certain unique marine environments.

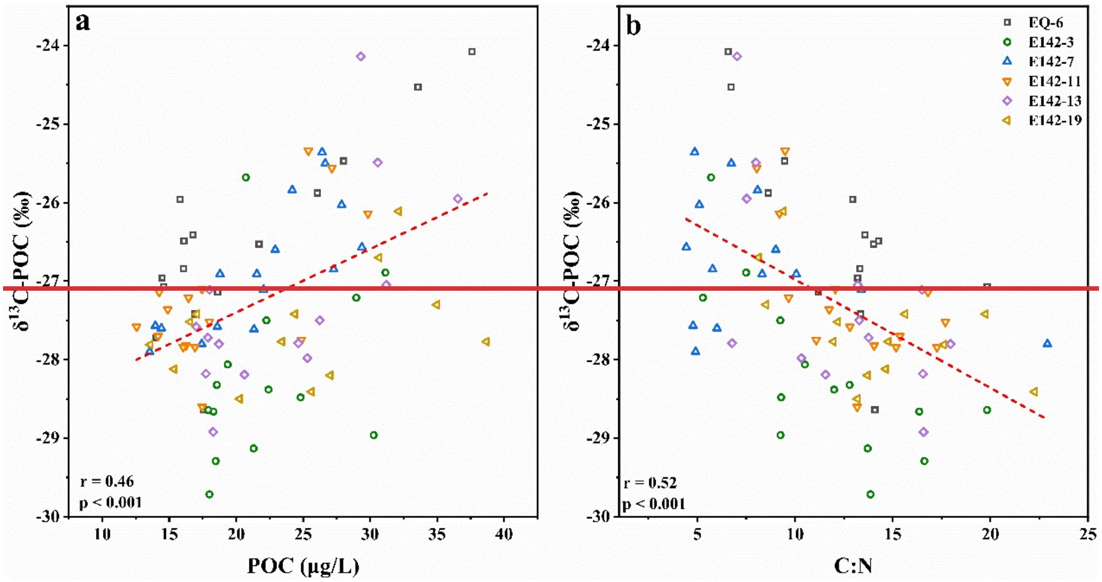

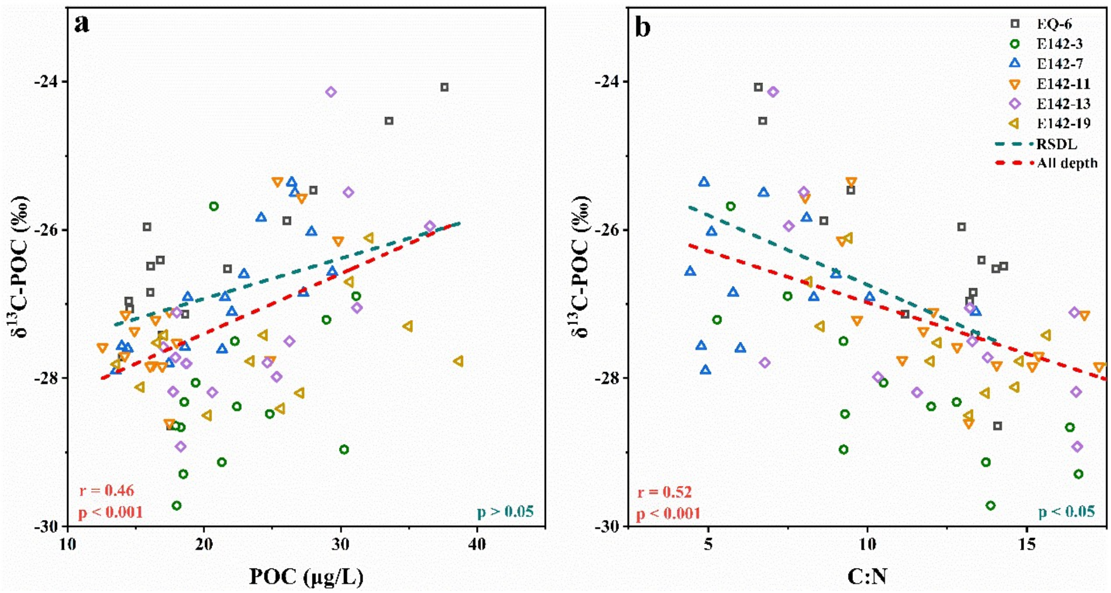

~~Figure 3~~Figure 4. a. Relationship between δ^{13}C-POC values and POC concentration; b. Relationship between δ^{13}C-POC values and C:N

3.3 Vertical distribution characteristics of DIC and δ^{13}C-DIC

Among the six stations, only the equatorial stations E143-13 and EQ-6 exhibited average upper DIC concentrations exceeding 2000 μmol/kg, with values of 2036 and 2054 μmol/kg, respectively. This phenomenon can be attributed to the fact that the surface water masses at these stations are composed of high-temperature and high-salinity ESW (Fig. 2). Although high temperatures generally hinder the dissolution of CO_2, they can accelerate the rate of CO_2 release by heterotrophic organisms. Meanwhile, high salinity increases the ionic strength and buffering capacity of seawater, promoting DIC accumulation (Zeebe and Wolf-Gladrow, 2001). These factors collectively contribute to the high DIC concentrations observed in the surface layers of these two stations. The average upper DIC concentration at station E142-19 was the next highest, reaching 1992 μmol/kg. This is due to upwelling at this station, which transports deep, high-DIC seawater to the middle ocean. Consequently, this station also recorded the highest average mid-layer DIC concentration among the six stations, at 2184 μmol/kg. Furthermore, since stations E142-3, E142-7, and E142-11 are predominantly influenced by the same water mass across all depths, their DIC concentrations are relatively similar at each depth (Fig. 5). The average DIC concentrations of all six stations in the upper ocean, middle ocean, and deep ocean were 2004 ± 65, 2147 ± 35, and 2234 ± 26 μmol/kg, respectively. There was a significant increase in DIC concentration from the upper to the deep ocean (~~Fig. 4~~Fig. 5). Affected by photosynthesis, DIC increases gradually in the upper ocean. In contrast, in the middle ocean, the rapid decomposition of POC released a large amount of inorganic carbon, causing a rapid increase in DIC throughout the water column. Then, in the deep ocean, a small amount of POC continues to degrade, while the release of DIC due to decreasing carbonate saturation with depth contributes to a gradual increase in DIC concentration within this layer.~~in deeper layers, only a tiny amount of POC continued to degrade, so the DIC concentration of this layer increased slowly.~~

Moreover, we observed surface δ^{13}C-DIC values ranging from -0.55 to 0.45‰ (average 0.12‰) in the research region, which is significantly lower than those reported in studies conducted in the Pacific region in the 1990s (Quay et al., 2017; Quay and Stutsman, 2003). This suggests that the ocean has absorbed more anthropogenic CO_2 as atmospheric CO_2 concentrations have increased over the years. The surface δ^{13}C-DIC value of station E142-11 was the lowest among the six stations, only -0.55‰, while the surface δ^{13}C-DIC value of station EQ-6 was the highest among the six stations, reaching 0.45‰. This is because station E142-11 was located at the strongest atmospheric CO_2 net sink area, while station EQ-6 was located at the atmospheric CO_2 net source area (Zhong et al., 2022). The sea-air exchange at station E142-11 was sufficient, leading to a lower δ^{13}C-DIC value in its surface water, as it was more likely to reach isotopic equilibrium with atmospheric CO_2. In contrast, the surface water of station EQ-6 was more susceptible to seawater mixing and biological primary production influences. The higher δ^{13}C-DIC values observed in the surface water of station EQ-6 can be attributed to the isotope fractionation caused by the consumption of a substantial amount of CO_2 by biological primary production (Quay et al., 2003). In analyzing the vertical distribution of δ^{13}C-DIC, the findings revealed a rapid decrease in δ^{13}C-DIC values at each station, mirroring the decline seen in δ^{13}C-POC values in the upper ocean (0-300 m) (Figs. 4, 5d). Within this depth range, the average decrease in δ^{13}C-POC values was 2.23‰, while the average decrease of δ^{13}C-DIC values was 0.30‰, with δ^{13}C-DIC reaching its minimum value in the subsurface. However, in the middle ocean layer (300-1,000 m), unlike δ^{13}C-POC, δ^{13}C-DIC values increased first and then stabilized (Fig. 4Fig. 5). Therefore, distinct differences exist in the overall change trends of δ^{13}C-DIC values and δ^{13}C-POC values in the ocean water column. Since the mutual conversion between POC and DIC was ongoing, this conversion process will inevitably cause changes in δ^{13}C-POC and δ^{13}C-DIC. Generally, the variation range of δ^{13}C-POC values was more significant than that of δ^{13}C-DIC, indicating the more complex biogeochemical processes experienced by POC (Meyer et al., 2016; Schmittner et al., 2013). This difference is also partly due to the much larger size of the DIC pool compared to the POC pool (Jeffrey et al., 1983). The high DIC concentration in the ocean buffers its isotopic variability, resulting in minimal changes in δ^{13}C-DIC values across the water column, whereas the smaller POC pool is more sensitive to localized biogeochemical processes, leading to greater variability in δ^{13}C-POC values.

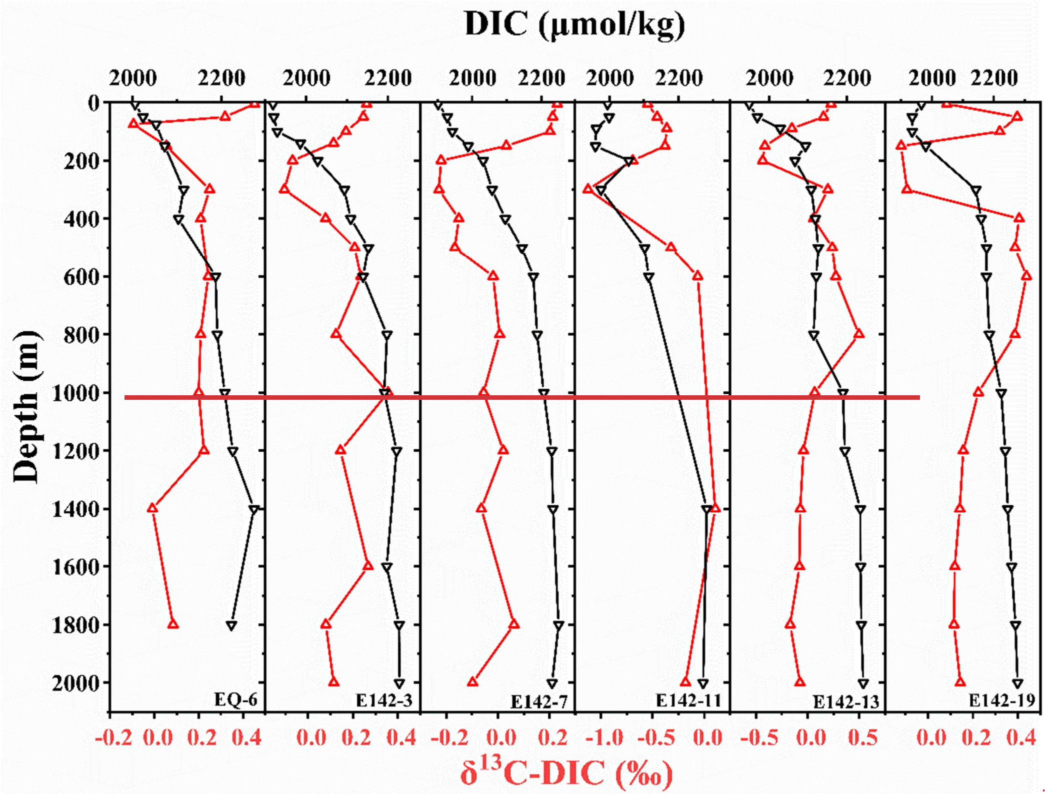

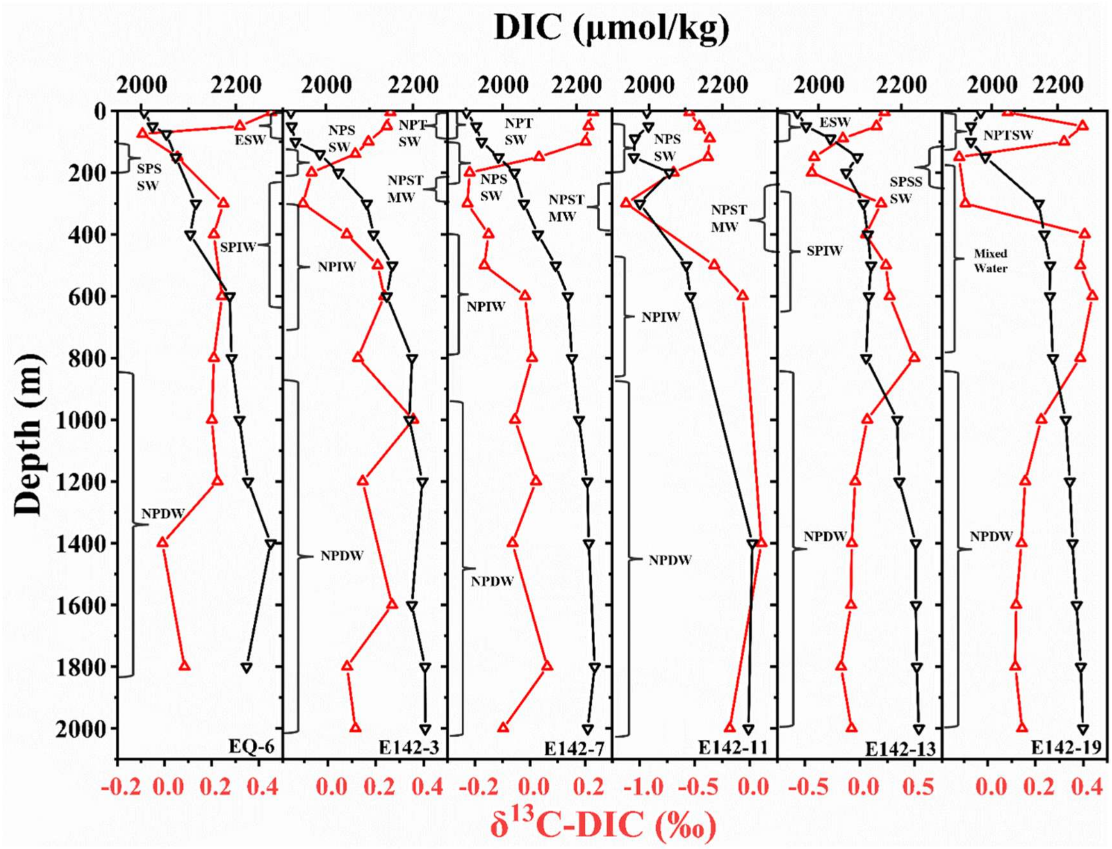

~~Figure 4~~Figure 5. Vertical distribution of DIC concentration and $\delta^{13}C$-DIC values at each sampling station. The black line represents DIC, and the red line represents $\delta^{13}C$-DIC values.

3.4 Transformation characteristics of POC in different water layers

According to the distribution characteristics of δ^{13}C-POC and δ^{13}C-DIC values, we divided the ocean water column into three biogeochemical layers: the POC rapid synthesis-degradation layer (RSDL, 0-300 m), the net degradation layer (NDL, 300-1,000 m) and the stable layer (SL, 1,000-2,000 m). Within the RSDL, POC was rapidly degraded while being synthesized. The synthesis of POC likely exceeded its degradation from the surface to the DCM layer, while the degradation of POC appeared to dominate below the DCM. The synthesis rate was greater than the degradation rate from the surface to the DCM layer, while the degradation rate was greater than the synthesis rate below the DCM, reflecting the rapid decrease in photosynthetic rate with depth. In this layer,In addition, the δ^{13}C-POC values and C:N in this layer exhibited a pronounced negative correlation., while no significant correlation is observed between δ^{13}C-POC values and POC concentration ($p > 0.05$) (Fig. 5Figs. 4a, 6a). Therefore, the rapid decrease of δ^{13}C-POC values in this layer was dominated by the selective degradation of POC and photosynthesisamino acids and carbohydrates. Both δ^{13}C-POC and δ^{13}C-DIC values decrease with increasing depth in the RSDL (Figs. 3, 5), and they exhibit a significant positive correlation within this layer (Fig. 6d). Although the degradation of POC typically lowers the δ^{13}C value of DIC, as the δ^{13}C value of POC is lower than that of DIC, the significant decline in δ^{13}C-DIC values observed in the RSDL, when considering the substantial difference in magnitude between the POC pool and the DIC pool, suggests the influence of additional processes. However, at the same time, δ^{13}C-POC and δ^{13}C-DIC showed a significant positive correlation in this layer (Fig. 5d). Supposing that POC underwent selective degradation, the resulting DIC should exhibit an enrichment in δ^{13}C. However, contrary to expectations, our findings indicate a decline in δ^{13}C-DIC within the RSDL. This perplexing occurrence can be attributed to two primary reasons. Specifically, On the one hand, the , phytoplankton and photosynthetic bacteria in the upper ocean tended to use the light $^{12}CO_2$ in the seawater for photosynthesis; thus the δ^{13}C-DIC values of the surface ocean at all stations was relatively high. However, light intensity diminishes with increasing depth, which is unfavorable for photosynthesis. This leads to the accumulation of $^{12}CO_2$ produced by the respiration of heterotrophic communities.However, light intensity diminished with depth increases, causing the photosynthesis rate to slow. Meanwhile, the respiration rate of the biological community was still very fast, resulting in the accumulation of light $^{12}CO_2$. Consequently, the δ^{13}C-DIC values in this layer steadily declined (Ge et al., 2022). In the NDL, sunlight was extremely weak, and photosynthesis was nearly absent. Heterotrophic communities dominate, leading to a continuous decrease in POC concentration and a corresponding increase in DIC concentration (Figs. 3, 5). Generally, the degradation of POC would be expected to lower the $\delta^{13}C$ value of DIC. However, in this layer, $\delta^{13}C$-POC values showed a significant negative correlation with both C:N and $\delta^{13}C$-DIC values (Fig. 6b, e), indicating the influence of additional processes on $\delta^{13}C$-DIC fractionation. The NDL often encompasses low-oxygen zones (Fig. 3), which are known to favor the activity of chemoautotrophic microorganisms. Compared to aerobic environments, the energy required for microorganisms to fix inorganic carbon into organic carbon is lower under low-oxygen condition (Hugler and Sievert, 2011; Mccollom and Amend, 2005). During this process, chemoautotrophic microorganisms preferentially utilize lighter ^{12}C isotopes, leading to the enrichment of ^{13}C in the remaining DIC pool. This microbial activity explains the observed increase in $\delta^{13}C$-DIC values in the NDL.~~In the NDL, the sunlight was pretty weak, and there was almost no photosynthesis. The rate of chemosynthesis of organic carbon was lower than the degradation rate of POC, causing the concentration of POC to continue decreasing. Additionally, the $\delta^{13}C$-POC in this layer showed a significant negative correlation with both C:N and $\delta^{13}C$-DIC (Fig. 5b, e), suggesting a very active mutual conversion process between POC and DIC. The large amount of selective degradation of amino acids and carbohydrate POC caused the $\delta^{13}C$-DIC in this layer to continue to increase.~~ In the SL, the POC concentration remained consistently low. $\delta^{13}C$-POC values did not correlate significantly with either C:N or $\delta^{13}C$-DIC (~~Fig. 5~~Fig. 6c, f). This was because the easily degradable components in POC had been completely consumed in the RSDL and NDL, and the remaining components were relatively refractory. As a result, the conversion of POC to DIC was rare in SL, leading to an absence of a clear link between $\delta^{13}C$-POC and $\delta^{13}C$-DIC.

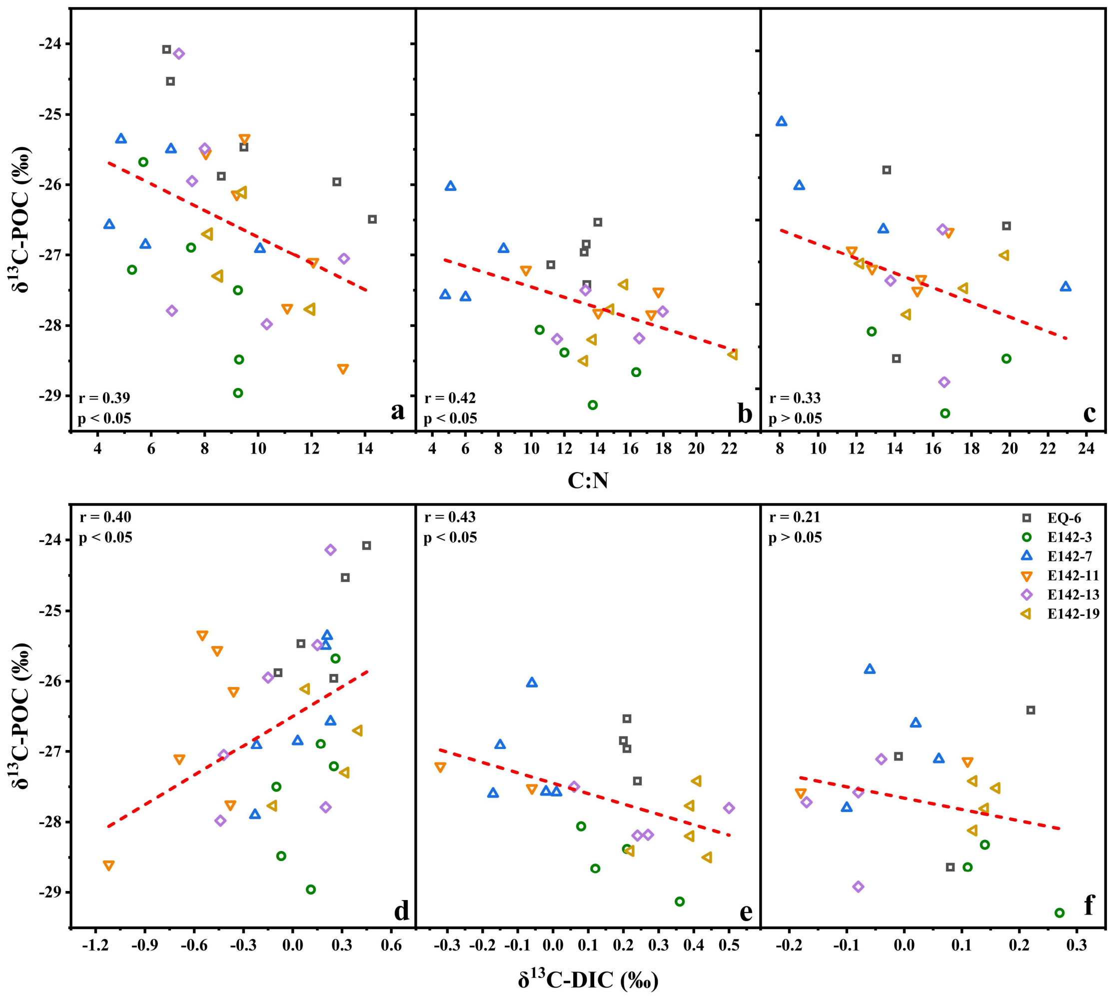

Figure 5Figure 6. Relationships between δ^{13}C-POC and C:N at different depths: (a) 0-300 m, (b) 300-1,000 m, (c) 1,000-2,000 m, and between δ^{13}C-POC and δ^{13}C-DIC at different depths: (d) 0-300 m, (e) 300-1,000 m, (f) 1,000-2,000 m.

4 Conclusions

In general, this study investigated the transformation characteristics of POC in the tropical northwest Pacific Ocean based on the δ^{13}C perspective. Our findings revealed three distinct stages of POC behavior in the ocean: rapid synthesis-degradation, net degradation, and stable existence. Below the RSDL, theThe selective degradation of POC dominated the changes in δ^{13}C-POC. The C:N ratio data in RSDL and NDL indicate an increase in the proportion of refractory lipids in POC, relative to more labile components such as amino acids and carbohydrates. Following vigorous selective degradation in the RSDL and NDL, an increase in the proportion of refractory lipids in POC was observed. Consequently, in the SL, POC was found to be stable with a slow degradation rate. The fractionation of δ^{13}C-DIC in the ocean is influenced by both the production and degradation processes of POC. Within the RSDL, δ^{13}C-DIC fractionation is predominantly governed by primary production, whereas within the NDL and SL, it is primarily influenced by the degradation process of POC.

Although we utilized δ^{13}C-POC and δ^{13}C-DIC to assess the overall transformation characteristics of POC, the specific synthesis and decomposition ratios of POC are still challenging to determine. Further research is needed on the monomer carbon isotopic composition of POC (lipids, amino acids, etc.) to enhance our understanding of the transformation process of POC.

Data Availability. The data files used in this paper are available at (Tian et al., 2024).

Competing interest. The authors declare that they have no conflict of interest.

Author contribution. Detong Tian: Investigation, Data Curation, Writing-original draft. Xuegang Li and Jinming Song: Conceptualization, Funding acquisition, Writing-review & editing. Jun Ma, Funding acquisition. Huamao Yuan, Liqin Duan,: Writing - Review & Editing.

Acknowledgments. This work was supported by the National Key Research and Development Program (grant no. 2022YFC3104305), National Natural Science Foundation of China (grant nos.42176200, 42206135); Laoshan Laboratory (grant nos. LSKJ202204001, LSKJ202205001). We appreciate the crews of the R/V *Kexue* for sampling assistance during the cruise of NORC2021-09 supported by the National Natural Science Foundation of China (project no. 42049909).

References

Brandt, P., Hahn, J., Schmidtko, S., Tuchen, F. P., Kopte, R., Kiko, R., Bourlès, B., Czeschel, R., and Dengler, M.: Atlantic Equatorial Undercurrent intensification counteracts warming-induced deoxygenation, Nat. Geosci., 14, 278-282, http://doi.org/10.1038/s41561-021-00716-1, 2021.

Bryan, J. R., Rlley, J. P., and Williams, P. J. L.: A winkler procedure for making precise measurements of oxygen concentration for productivity and related studies, Journal of Experimental Marine Biology and Ecology, 21, 191-197, http://doi.org/10.1016/0022-0981 (76)90114-3, 1976.

Buesseler, K. O., Boyd, P. W., Black, E. E., and Siegel, D. A.: Metrics that matter for assessing the ocean biological carbon pump, Proc Natl Acad Sci U S A, 117, 9679-9687, http://doi.org/10.1073/pnas.1918114117, 2020.

Close, H. G. and Henderson, L. C.: Open-Ocean Minima in $\delta^{13}C$ Values of Particulate Organic Carbon in the Lower Euphotic Zone, Front. Mar. Sci., 7, http://doi.org/10.3389/fmars.2020.540165, 2020.

Close, H. G., Wakeham, S. G., and Pearson, A.: Lipid and ^{13}C signatures of submicron and suspended particulate organic matter in the Eastern Tropical North Pacific: Implications for the contribution of Bacteria, Deep Sea Res. Part I Oceanogr. Res. Pap., 85, 15-34, http://doi.org/10.1016/j.dsr.2013.11.005, 2014.

Ding, L., Qi, Y., Shan, S., Ge, T., Luo, C., and Wang, X.: Radiocarbon in Dissolved Organic and Inorganic Carbon of the South China Sea, J. Geophys. Res. Oceans, 125, http://doi.org/10.1029/2020jc016073, 2020.

Druffel, E. R. M., Bauer, J. E., Griffin, S., and Hwang, J.: Penetration of anthropogenic carbon into organic particles of the deep ocean, Geophys. Res. Lett., 30, http://doi.org/10.1029/2003gl017423, 2003.

Eadie, B. J. and Jeffrey, L. M.: $\delta^{13}C$ analyses of oceanic particulate organic matter, Mar. Chem., 1, 199-209, http://doi.org/10.1016/0304-4203 (73)90004-2, 1973.

Friedlingstein, P., O'Sullivan, M., Jones, M. W., Andrew, R. M., Bakker, D. C. E., Hauck, J., Landschützer, P., Le Quéré, C., Luijkx, I. T., Peters, G. P., Peters, W., Pongratz, J., Schwingshackl, C., Sitch, S., Canadell, J. G., Ciais, P., Jackson, R. B., Alin, S. R., Anthoni, P., Barbero, L., Bates, N. R., Becker, M., Bellouin, N., Decharme, B., Bopp, L., Brasika, I. B. M., Cadule, P., Chamberlain, M. A., Chandra, N., Chau, T.-T.-T., Chevallier, F., Chini, L. P., Cronin, M., Dou, X., Enyo, K., Evans, W., Falk, S., Feely, R. A., Feng, L., Ford, D. J., Gasser, T., Ghattas, J., Gkritzalis, T., Grassi, G., Gregor, L., Gruber, N., Gürses, Ö., Harris, I., Hefner, M., Heinke, J., Houghton, R. A., Hurtt, G. C., Iida, Y., Ilyina, T., Jacobson, A. R., Jain, A., Jarníková, T., Jersild, A., Jiang, F., Jin, Z., Joos, F., Kato, E., Keeling, R. F., Kennedy, D., Klein Goldewijk, K., Knauer, J., Korsbakken, J. I., Körtzinger, A., Lan, X., Lefèvre, N., Li, H., Liu, J., Liu, Z., Ma, L., Marland, G., Mayot, N., McGuire, P. C., McKinley, G. A., Meyer, G., Morgan, E. J., Munro, D. R., Nakaoka, S.-I., Niwa, Y., O'Brien, K. M., Olsen, A., Omar, A. M., Ono, T., Paulsen, M., Pierrot, D., Pocock, K., Poulter, B., Powis, C. M., Rehder, G., Resplandy, L., Robertson, E., Rödenbeck, C., Rosan, T. M., Schwinger, J., Séférian, R., Smallman, T. L., Smith, S. M., Sospedra-Alfonso, R., Sun, Q., Sutton, A. J., Sweeney, C., Takao, S., Tans, P. P., Tian, H., Tilbrook, B., Tsujino, H., Tubiello, F., van der Werf, G. R., van Ooijen, E., Wanninkhof, R., Watanabe, M., Wimart-Rousseau, C., Yang, D., Yang, X., Yuan, W., Yue, X., Zaehle, S., Zeng, J., and Zheng, B.: Global Carbon Budget 2023, Earth Syst. Sci. Data, 15, 5301-5369, http://doi.org/10.5194/essd-15-5301-2023, 2023.

Gao, W., Wang, Z., Li, X., and Huang, H.: The increased storage of suspended particulate matter in the upper water of the tropical Western Pacific during the 2015/2016 super El Niño event, J. Oceanol.

Limnol., 39, 1675-1689, http://doi.org/10.1007/s00343-021-0362-0, 2021.
Ge, T., Luo, C., Ren, P., Zhang, H., Fan, D., Chen, H., Chen, Z., Zhang, J., and Wang, X.: Stable carbon isotopes of dissolved inorganic carbon in the Western North Pacific Ocean: Proxy for water mixing and dynamics, Front. Mar. Sci., 9, http://doi.org/10.3389/fmars.2022.998437, 2022.
Guo, J., Zhou, B., Achterberg, E. P., Yuan, H., Song, J., Duan, L., and Li, X.: Rapid Cycling of Bacterial Particulate Organic Matter in the Upper Layer of the Western Pacific Warm Pool, Geophys. Res. Lett., 50, http://doi.org/10.1029/2023gl102896, 2023a.
Guo, J., Achterberg, E. P., Shen, Y., Yuan, H., Song, J., Liu, J., Li, X., and Duan, L.: Stable carbon isotopic composition of amino sugars in heterotrophic bacteria and phytoplankton: Implications for assessment of marine organic matter degradation, Limnology and Oceanography, 68, 2814-2825, http://doi.org/10.1002/lno.12468, 2023b.
Häggi, C., Pätzold, J., Bouillon, S., and Schefuß, E.: Impact of selective degradation on molecular isotope compositions in oxic and anoxic marine sediments, Org. Geochem., 153, http://doi.org/10.1016/j.orggeochem.2021.104192, 2021.
Hayes, J. M.: Factors controlling ^{13}C contents of sedimentary organic compounds: Principles and evidence, Mar. Geol., 113, 111-125, http://doi.org/10.1016/0025-3227 (93)90153-m, 1993.
Henderson, L. C., Wittmers, F., Carlson, C. A., Worden, A. Z., and Close, H. G.: Variable carbon isotope fractionation of photosynthetic communities over depth in an open-ocean euphotic zone, Proc Natl Acad Sci U S A, 121, e2304613121, http://doi.org/10.1073/pnas.2304613121, 2024.
Herndl, G. J., Bayer, B., Baltar, F., and Reinthaler, T.: Prokaryotic Life in the Deep Ocean's Water Column, Ann Rev Mar Sci, 15, 461-483, http://doi.org/10.1146/annurev-marine-032122-115655, 2023.
Hernes, P. J. and Benner, R.: Transport and diagenesis of dissolved and particulate terrigenous organic matter in the North Pacific Ocean, Deep Sea Res. Part I Oceanogr. Res. Pap., 49, 2119-2132, http://doi.org/10.1016/s0967-0637 (02)00128-0, 2002.
Hu, D., Wu, L., Cai, W., Gupta, A. S., Ganachaud, A., Qiu, B., Gordon, A. L., Lin, X., Chen, Z., Hu, S., Wang, G., Wang, Q., Sprintall, J., Qu, T., Kashino, Y., Wang, F., and Kessler, W. S.: Pacific western boundary currents and their roles in climate, Nature, 522, 299-308, http://doi.org/10.1038/nature14504, 2015.
Hugler, M. and Sievert, S. M.: Beyond the Calvin cycle: autotrophic carbon fixation in the ocean, Ann Rev Mar Sci, 3, 261-289, http://doi.org/10.1146/annurev-marine-120709-142712, 2011.
Hwang, J. and Druffel, E. R.: Lipid-like material as the source of the uncharacterized organic carbon in the ocean?, Science, 299, 881-884, http://doi.org/10.1126/science.1078508, 2003.
Hwang, J., Druffel, E. R. M., Eglinton, T. I., and Repeta, D. J.: Source (s) and cycling of the nonhydrolyzable organic fraction of oceanic particles, Geochim. Cosmochim. Acta, 70, 5162-5168, http://doi.org/10.1016/j.gca.2006.07.020, 2006.
Iversen, M. H. and Ploug, H.: Temperature effects on carbon-specific respiration rate and sinking velocity of diatom aggregates – potential implications for deep ocean export processes, Biogeosciences, 10, 4073-4085, http://doi.org/10.5194/bg-10-4073-2013, 2013.
Jeffrey, A. W. A., Pflaum, R. C., Brooks, J. M., and Sackett, W. M.: Vertical trends in particulate organic carbon ^{13}C: ^{12}C ratios in the upper water column, Deep Sea Research Part A. Oceanographic Research Papers, 30, 971-983, http://doi.org/10.1016/0198-0149 (83)90052-3, 1983.
Jia, Q., Li, T., Xiong, Z., Steinke, S., Jiang, F., Chang, F., and Qin, B.: Hydrological variability in the western tropical Pacific over the past 700 kyr and its linkage to Northern Hemisphere climatic change, Palaeogeogr. Palaeoclimatol. Palaeoecol., 493, 44-54,

http://doi.org/10.1016/j.palaeo.2017.12.039, 2018.
Kharbush, J. J., Close, H. G., Van Mooy, B. A. S., Arnosti, C., Smittenberg, R. H., Le Moigne, F. A. C., Mollenhauer, G., Scholz-Böttcher, B., Obreht, I., Koch, B. P., Becker, K. W., Iversen, M. H., and Mohr, W.: Particulate Organic Carbon Deconstructed: Molecular and Chemical Composition of Particulate Organic Carbon in the Ocean, Front. Mar. Sci., 7, http://doi.org/10.3389/fmars.2020.00518, 2020.
Lee, C., Wakeham, S. G., and I. Hedges, J.: Composition and flux of particulate amino acids and chloropigments in equatorial Pacific seawater and sediments, Deep Sea Res. Part I Oceanogr. Res. Pap., 47, 1535-1568, http://doi.org/10.1016/s0967-0637 (99)00116-8, 2000.
Longhurst, A. R. and Glen Harrison, W.: The biological pump: Profiles of plankton production and consumption in the upper ocean, Prog. Oceanogr., 22, 47-123, http://doi.org/10.1016/0079-6611 (89)90010-4, 1989.
Ma, J., Song, J., Li, X., Yuan, H., Li, N., Duan, L., and Wang, Q.: Control factors of DIC in the Y3 seamount waters of the Western Pacific Ocean, J. Oceanol. Limnol., 38, 1215-1224, http://doi.org/10.1007/s00343-020-9314-3, 2020.
Ma, J., Song, J., Li, X., Wang, Q., Zhong, G., Yuan, H., Li, N., and Duan, L.: The OMZ and Its Influence on POC in the Tropical Western Pacific Ocean: Based on the Survey in March 2018, Front. Earth Sci., 9, http://doi.org/10.3389/feart.2021.632229, 2021.
McCollom, T. M. and Amend, J. P.: A thermodynamic assessment of energy requirements for biomass synthesis by chemolithoautotrophic micro-organisms in oxic and anoxic environments, Geobiology, 3, 135-144, http://doi.org/10.1111/j.1472-4669.2005.00045.x, 2005.
Meyer, K. M., Ridgwell, A., and Payne, J. L.: The influence of the biological pump on ocean chemistry: implications for long-term trends in marine redox chemistry, the global carbon cycle, and marine animal ecosystems, Geobiology, 14, 207-219, http://doi.org/10.1111/gbi.12176, 2016.
Morales, M., Aflalo, C., and Bernard, O.: Microalgal lipids: A review of lipids potential and quantification for 95 phytoplankton species, Biomass and Bioenergy, 150, http://doi.org/10.1016/j.biombioe.2021.106108, 2021.
Owens, S. A., Pike, S., and Buesseler, K. O.: Thorium-234 as a tracer of particle dynamics and upper ocean export in the Atlantic Ocean, Deep Sea Res. Part II Top. Stud. Oceanogr., 116, 42-59, http://doi.org/10.1016/j.dsr2.2014.11.010, 2015.
Passos, J. G., Soares, L. F., Sumida, P. Y. G., Bendia, A. G., Nakamura, F. M., Pellizari, V. H., and Signori, C. N.: Contribution of chemoautotrophy and heterotrophy to the microbial carbon cycle in the Southwestern Atlantic Ocean, Ocean Coast. Res., 70, http://doi.org/10.1590/2675-2824070.22137jgp, 2022.
Quay, P. and Stutsman, J.: Surface layer carbon budget for the subtropical N. Pacific: constraints at station ALOHA, Deep Sea Res. Part I Oceanogr. Res. Pap., 50, 1045-1061, http://doi.org/10.1016/s0967-0637 (03)00116-x, 2003.
Quay, P., Sonnerup, R., Munro, D., and Sweeney, C.: Anthropogenic CO_2 accumulation and uptake rates in the Pacific Ocean based on changes in the $^{13}C/^{12}C$ of dissolved inorganic carbon, Glob. Biogeochem. Cycles, 31, 59-80, http://doi.org/10.1002/2016gb005460, 2017.
Quay, P., Sonnerup, R., Westby, T., Stutsman, J., and McNichol, A.: Changes in the $^{13}C/^{12}C$ of dissolved inorganic carbon in the ocean as a tracer of anthropogenic CO_2 uptake, Glob. Biogeochem. Cycles, 17, http://doi.org/10.1029/2001gb001817, 2003.
Radenac, M.-H., Messié, M., Léger, F., and Bosc, C.: A very oligotrophic zone observed from space in

the equatorial Pacific warm pool, Remote Sens. Environ., 134, 224-233, http://doi.org/10.1016/j.rse.2013.03.007, 2013.

Reinthaler, T., van Aken, H. M., and Herndl, G. J.: Major contribution of autotrophy to microbial carbon cycling in the deep North Atlantic's interior, Deep Sea Res. Part II Top. Stud. Oceanogr., 57, 1572-1580, http://doi.org/10.1016/j.dsr2.2010.02.023, 2010.

Sannigrahi, P., Ingall, E. D., and Benner, R.: Cycling of dissolved and particulate organic matter at station Aloha: Insights from ^{13}C NMR spectroscopy coupled with elemental, isotopic and molecular analyses, Deep Sea Res. Part I Oceanogr. Res. Pap., 52, 1429-1444, http://doi.org/10.1016/j.dsr.2005.04.001, 2005.

Schmittner, A., Gruber, N., Mix, A. C., Key, R. M., Tagliabue, A., and Westberry, T. K.: Biology and air–sea gas exchange controls on the distribution of carbon isotope ratios (δ¹³C) in the ocean, Biogeosciences, 10, 5793-5816, http://doi.org/10.5194/bg-10-5793-2013, 2013.

Schönau, M. C., Rudnick, D. L., Gopalakrishnan, G., Cornuelle, B. D., and Qiu, B.: Mean, Annual, and Interannual Circulation and Volume Transport in the Western Tropical North Pacific From the Western Pacific Ocean State Estimates (WPOSE), J. Geophys. Res. Oceans, 127, http://doi.org/10.1029/2021jc018213, 2022.

Schouten, S., Klein Breteler, W. C. M., Blokker, P., Schogt, N., Rijpstra, W. I. C., Grice, K., Baas, M., and Sinninghe Damsté, J. S.: Biosynthetic effects on the stable carbon isotopic compositions of algal lipids: implications for deciphering the carbon isotopic biomarker record, Geochim. Cosmochim. Acta, 62, 1397-1406, http://doi.org/10.1016/s0016-7037 (98)00076-3, 1998.

Smith, C. R., De Leo, F. C., Bernardino, A. F., Sweetman, A. K., and Arbizu, P. M.: Abyssal food limitation, ecosystem structure and climate change, Trends Ecol Evol, 23, 518-528, http://doi.org/10.1016/j.tree.2008.05.002, 2008.

Song, J.: Biogeochemical Processes of Biogenic Elements in China Marginal Seas, Advanced Topics in Science and Technology in China, Springer Berlin, Heidelberg, 662 pp., http://doi.org/https://doi.org/10.1007/978-3-642-04060-3, 2010.

Sun, Q., Song, J., Li, X., Yuan, H., and Wang, Q.: The bacterial diversity and community composition altered in the oxygen minimum zone of the Tropical Western Pacific Ocean, J. Oceanol. Limnol., 39, 1690-1704, http://doi.org/10.1007/s00343-021-0370-0, 2021.

Takahashi, T., Sutherland, S. C., Wanninkhof, R., Sweeney, C., Feely, R. A., Chipman, D. W., Hales, B., Friederich, G., Chavez, F., Sabine, C., Watson, A., Bakker, D. C. E., Schuster, U., Metzl, N., Yoshikawa-Inoue, H., Ishii, M., Midorikawa, T., Nojiri, Y., Körtzinger, A., Steinhoff, T., Hoppema, M., Olafsson, J., Arnarson, T. S., Tilbrook, B., Johannessen, T., Olsen, A., Bellerby, R., Wong, C. S., Delille, B., Bates, N. R., and de Baar, H. J. W.: Climatological mean and decadal change in surface ocean pCO_2, and net sea–air CO_2 flux over the global oceans, Deep Sea Res. Part II Top. Stud. Oceanogr., 56, 554-577, http://doi.org/10.1016/j.dsr2.2008.12.009, 2009.

Thompson, R. O. R. Y.: Climatological Numerical Models of the Surface Mixed Layer of the Ocean, Journal of Physical Oceanography, 6, 496-503, 1976.

Tian, D., Li, X., Song, J., Ma, J, Yuan, H & Duan, L.: Vertical layering and transformation of particulate organic carbon in the tropical Northwestern Pacific Ocean waters based on δ13C, Figshare [Dataset]. https://doi.org/10.6084/m9.figshare.26197808, 2024

Turner, J. T.: Zooplankton fecal pellets, marine snow, phytodetritus and the ocean's biological pump, Prog. Oceanogr., 130, 205-248, http://doi.org/10.1016/j.pocean.2014.08.005, 2015.

Walsh, D. A., Zaikova, E., Howes, C. G., Song, Y. C., Wright, J. J., Tringe, S. G., Tortell, P. D., and Hallam, S. J.: Metagenome of a versatile chemolithoautotroph from expanding oceanic dead zones, Science, 326, 578-582, http://doi.org/10.1126/science.1175309, 2009.

Wu, L., Liu, Z., Liu, Y., Liu, Q., and Liu, X.: Potential global climatic impacts of the North Pacific Ocean, Geophys. Res. Lett., 32, http://doi.org/10.1029/2005gl024812, 2005.

Zeebe, R. E. and Wolf-Gladrow, D.: CO_2 in Seawater: Equilibrium, Kinetics, Isotopes, Elsevier Science2001.

Zhong, G., Li, X., Song, J., Qu, B., Wang, F., Wang, Y., Zhang, B., Tian, D., Ma, J., Yuan, H., Duan, L., Li, N., Wang, Q., and Xing, J.: The increasing big gap of carbon sink between the western and eastern Pacific in the last three decades, Front. Mar. Sci., 9, http://doi.org/10.3389/fmars.2022.1088181, 2022.

Zuo, J., Song, J., Yuan, H., Li, X., Li, N., and Duan, L.: Impact of Kuroshio on the dissolved oxygen in the East China Sea region, J. Oceanol. Limnol., 37, 513-524, http://doi.org/10.1007/s00343-019-7389-5, 2018.